





Biological effects of vanillic acid. *iso*-vanillic acid. and *orto*-vanillic acid as environmental pollutants

Marzena Matejczyk ^a  , Piotr Ofman ^b, Edyta Juszczyk-Kubiak ^c, Renata Świsłocka ^a, Wong Ling Shing ^d, Kavindra Kumar Kesari ^e, Balu Prakash ^f, Włodzimierz Lewandowski ^a

Show more 

 Outline |  Share  Cite

<https://doi.org/10.1016/j.ecoenv.2024.116383> ↗

[Get rights and content](#) ↗

Under a Creative Commons [license](#) ↗

open access

Highlights

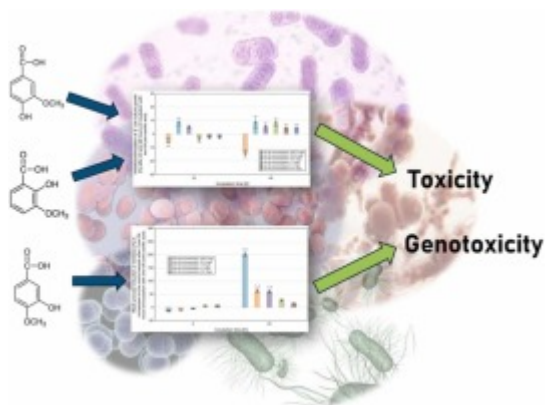
- VA and its isomers (*iso*-VA and *orto*-VA) have antimicrobial activity.
- VA and its isomers are toxic and genotoxic.
- VA and its isomers have the potential to generate oxidative stress.
- VA isomerism affects its biological activity.

Abstract

Vanillic acid (4-hydroxy-3-methoxybenzoic acid) (VA) is a natural benzoic acid derivative commonly found in herbs, rice, maize, and some fruits and vegetables.

However, due to the wide use of VA in various industrial sectors, its presence in the environment might harm living organisms. This study evaluated the toxicity of VA and its isomers, *iso*-VA and *orto*-VA. Firstly, the antimicrobial effect of VA and its isomers *iso*-VA and *orto*-VA (in doses of 1000; 100, 10, 1; 0.1; 0.01 mg/L) against *Escherichia coli*, *Sarcina spp.*, *Enterobacter homaechei*, *Staphylococcus aureus* and *Candida albicans* were identified. The toxic effect and protein degradation potential of VA and its isomers were determined using *E. coli grpE:lucCDABE* and *lac:lucCDABE* biosensor strains. However, the genotoxicity and oxidative stress generation were assessed with the *E. coli recA:lucCDABE* biosensor and *E. coli* strain. The results showed that VA, *iso*-VA, and *orto*-VA exhibited antimicrobial activity against all tested bacterial strains. However, VA's antimicrobial effect differed from *iso*-VA and *orto*-VA. Similar toxic, genotoxic, and oxidative stress-inducing effects were observed for VA and its isomers. Each compound exhibited toxicity, cellular protein degradation, and genotoxic activity against *E. coli grpE:lucCDABE*, *E. coli lac:lucCDABE*, and *E. coli recA:lucCDABE* strains. Analysis of reactive oxygen species (ROS) generation within *E. coli* cells highlighted oxidative stress as a contributing factor to the toxicity and genotoxicity of VA and its isomers. While the findings suggest potential applications of VA compounds as food preservatives, their presence in the environment raises concerns regarding the risks posed to living organisms due to their toxic and genotoxic characteristics.

Graphical Abstract



Download: [Download high-res image \(135KB\)](#)

Download: [Download full-size image](#)



Previous

Next



Keywords

Vanillic acid; Toxicity; Microbial biosensor strains; Water pollutants; Clean water

1. Introduction

Vanillic acid (4-hydroxy-3-methoxybenzoic acid) (VA) is a benzoic acid derivative. It is a naturally occurring aromatic phenolic acid found in various herbs such as Angelica Sinensis, Ocimum basilicum, Origanum vulgare, Salvia Rosmarinus, and Thymus vulgaris, as well as in cereals like rice and maize. VA is also present in fruits and vegetables, such as Euterpe oleracea, Phoenix dactylifera and Olea europaea fruits and beverages like green tea ([Świsłocka et al., 2013](#), [Kaur et al., 2022](#), [Oke et al., 2021](#), [Sha et al., 2023](#)). Numerous scientific studies have demonstrated the diverse pharmacological properties of VA, including its anti-venom, anti-inflammatory, antimicrobial, cardioprotective, hepatoprotective, free radical scavenging, and antioxidant activities ([Tanaka et al., 2019](#), [Girawale et al., 2022](#), [Caetano et al., 2023](#), [Shabani et al., 2023](#)). VA has shown efficacy as an antimicrobial compound against foodborne bacteria such as S. aureus, E. coli, and carbapenem-resistant E. cloacae ([Qian et al., 2019](#)). The *in vivo* anti-diabetic properties of VA have been reported by [Sha et al. \(2023\)](#). In rats, VA reduced blood glucose and triglyceride levels and improved insulin resistance, glucose tolerance and insulin signalling. In several studies, the anticancer potency of VA, including lung cancer, prostate cancer, liver cancer, melanoma, and endometrial carcinoma, has been reported ([Kaur et al., 2021](#)). Moreover, VA has pharmacological activity in treating inflammatory, metabolic, bone loss, and neurodegenerative diseases ([Girawale et al., 2022](#), [Sha et al., 2023](#)). VA has also found applications in brovanexine, vanitiolide, etamivan and flecainide production. The protective properties of VA on human skin exposed to UV radiation and premature skin ageing were also demonstrated; VA is added to ointments, lotions, and creams ([Zilius et al., 2013](#), [Girawale et al., 2022](#)). Additionally, VA is used as a fragrance, an additive, a flavouring, and a colouring agent ([Victor-Ortega et al., 2022](#)). Currently, VA is used in pharmaceutical, food, flavour, cosmetic, polymer, and wine-making industries and the synthesis of biobased polymers. VA is extensively produced in the industry through chemical synthesis and microbial enzymatic processes ([Girawale et al., 2022](#)). The demand for VA has been steadily rising, particularly in Europe and China. Between 2012 and 2016, global production of VA increased from 18.6 MT to 18.9 MT, showing an average growth rate of 1.6% ([Girawale et al., 2022](#)). The constantly increasing consumption of VA leads to its presence in wastewater. Moreover, VA enters wastewater as a metabolic by-product of caffeic acid. VA is frequently detected in the urine of individuals who consume coffee, chocolate, tea, and vanilla-flavoured confectionery ([Dhananjaya et al., 2006](#)).

According to the US Environmental Protection Agency (EPA), the permissible concentration limit of discharge for effluents containing phenolic compounds is 1 mg/L. However, the allowable limit for phenol content in potable water set by the World Health Organization (WHO) is 0.002 mg/L ([Victor-Ortega et al., 2022](#)). Despite the standard given by EPA and WHO, the content of phenolic compounds in industrial and domestic wastewaters could be many times higher than the allowed concentration. For example, coffee wastewaters might range from 12 to 388 mg/L, polyphenol content detected in winery wastewaters ranged from 0.5 to 1450 mg/L, and the total phenolics in olive mill wastewaters ranged from 0.03 to 10 g/L ([Ramos et al., 2023](#)).

Numerous significant biodegradation metabolites of VA have been identified to date, including o-dihydroxybenzene, butyric acid, valproic acid, and guaiaicol; some of these are harmful to living organisms ([Wang et al., 2018](#)). Therefore, further research on the toxicity of VA towards living organisms is warranted. Currently, there is a lack of studies examining the biological effects of VA isomers such as *iso*-VA and *orto*-VA. The existing scientific literature only reports the detection of general VA in wastewater, with no information on the presence of its *iso*- and *orto*-isomers as environmental contaminants. Nevertheless, this absence of data does not preclude the potential occurrence of VA isomers as micropollutants.

In this study, we compared the biological properties of vanillic acid (VA) and its isomeric forms, *iso*-vanillic acid (*iso*-VA) and *orto*-vanillic acid (*orto*-VA). We investigated their antimicrobial activity, toxicity, cytotoxicity, genotoxicity, and ability to induce oxidative stress. Antimicrobial activity was assessed using various bacterial strains, including *Escherichia coli* ATCC-25922, Sarcina spp. ATCC-35659, Enterobacter homaechei LBM ATCC-700323, *Staphylococcus aureus* ATCC-25923, and Candida albicans ATCC-10231. To evaluate toxicity, protein damage, and genotoxicity, we employed three distinct bioluminescent *E. coli* biosensor strains. These strains carried promoters for *recA* (indicating DNA damage and genotoxicity), *grpE* (indicating toxicity and protein damage), and *lac* (indicating constitutive expression and toxicity), fused to the bacterial operon luxCDABE from Photobacterium luminescens. Additionally, we quantified reactive oxygen species (ROS) production in *E. coli* cultures to measure the level of oxidative stress induced by exposure to the tested chemical compounds.

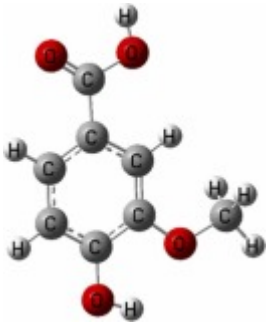
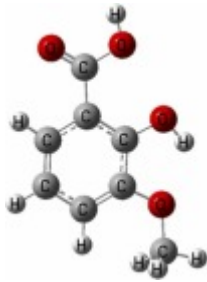
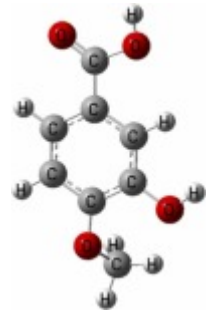
2. Materials and methods

2.1. Chemical compounds

VA, *iso*-VA, and *orto*-VA were purchased from Sigma-Aldrich (Sigma-Aldrich, UK). All chemicals were dissolved in dimethyl sulfoxide (DMSO). To minimize the impact of

DMSO on bacterial cells, tested chemical compound solutions were diluted in 0.86% NaCl in a ratio of 1:9 (100 μ L DMSO and 900 μ L 0.86% NaCl). *VA*, *iso-VA*, and *orto-VA* were tested at concentrations of 0.01, 0.1, 1, 10 and 100 mg/L. The concentration of 1000 mg/L was also tested to determine the antimicrobial activity. In each well of a 96-well plate, the tested samples comprised 100 μ l of microorganism culture and 100 μ l of the respective concentration of VA, *iso-VA*, and *orto-VA* dissolved in a mixture of DMSO and 0.86% NaCl at a ratio of 1:9 (100 μ l DMSO and 900 μ l 0.86% NaCl). The control samples lacked the tested chemical compounds. They were composed of equivalent amounts of microorganism cultures and solvents as the test samples corresponding to the specified concentrations of the chemicals under investigation. The concentrations of the tested compounds were selected based on the polyphenol concentrations found in wastewater, as reported by [Yanez et al. \(2016\)](#) and [Ramos et al. \(2023\)](#). Additionally, the study aimed to explore the performance of the microbial biosensors *E. coli* *grpE:lucCDABE*, *E. coli* *lac:lucCDABE*, and *E. coli* *recA:lucCDABE* across a range of concentrations, including lower concentrations (0.1 and 0.01, 1, 10 mg/L) and higher concentrations (100 mg/L). The physical and chemical properties of the tested acids are presented in [Table 1](#).

Table 1. Chemical and physical properties of VA, *iso-VA* and *orto-VA*.

Nazwa	Vanillic acid (VA)	Ortovanillic acid (orto-VA)	Isovanillic acid (iso-VA)
Chemical structure			
IUPAC name	4-hydroxy-3-methoxybenzoic acid	2-hydroxy-3-methoxybenzoic acid	3-hydroxy-4-methoxybenzoic acid
Molecular Weight [g/mol]	168.15	168.15	168.15
Appearance	Light yellow to yellow to orange powder	Light brown powder	Beige to gray-brown powder
Melting Point [°C]	173–177	147–150	250–253

Nazwa	Vanillic acid (VA)	Ortovanillic acid (orto-VA)	Isovanillic acid (iso-VA)
Solubility in H₂O	1.5 g/L w temp. 14 °C	3.86 g/L	4.42 g/L
pKa	4.53	2.85	4.35
XLogP3	1.4	1.9	1.4
Acute toxicity LD₅₀	Intraperitoneal, 5020 mg/kg (rat), >2691 mg/kg (mouse)	Intraperitoneal, 2056 mg/kg (rat),	Intraperitoneal, 2974 mg/kg (rat)
	PubChem Compound Summary for CID 8468, vanillic acid. Retrieved July 6, 2023 from https://pubchem.ncbi.nlm.nih.gov/compound/Vanillic-Acid ↗	PubChem Compound Summary for CID 70140, 2-hydroxy-3-methoxybenzoic acid. Retrieved July 6, 2023 from https://pubchem.ncbi.nlm.nih.gov/compound/2-Hydroxy-3-methoxybenzoic-acid ↗	PubChem Compound Summary for CID 12575, 3-Hydroxy-4-methoxybenzoic acid. Retrieved July 6, 2023 from https://pubchem.ncbi.nlm.nih.gov/compound/3-Hydroxy-4-methoxybenzoic-acid ↗

2.2. The preparation of microorganisms

For antimicrobial activity, five different strains (*E. coli* ATCC-25922, *Sarcina* spp., ATCC-35659, *E. homaechei* LBM ATCC-700323, *S. aureus* ATCC-25923 and *C. albicans* ATCC-1023) representing bacteria and fungi were purchased from ATCC (American Type Culture Collection, USA). *E. coli* RFM443 strains with a plasmid transcriptional fusion of *grpE* and *lac* promoters with *luxCDABE* reporter gene were applied to determine toxicity and protein damage potency of VA, iso-VA, and orto-VA. The utilization of bioluminescent microbial biosensors to estimate the toxicity of different micropollutants, including pharmaceuticals and their metabolites, as well as compounds of natural origin, has been reported in several studies (Bae et al., 2020, Rojas-Villacorta et al., 2022a, Rojas-Villacorta et al., 2022b, Matejczyk et al., 2023). In this study, for genotoxicity of VA, iso-VA and orto-VA, the *E. coli* RFM443 *recA:luxCDABE* strain with genotoxin-sensitive *recA* promoter was utilized (Melamed et al., 2012, Zhu et al., 2022, Rojas-Villacorta et al., 2022a, Rojas-Villacorta et al., 2022b). The *E. coli* strains were obtained from the laboratory collection of microorganisms of Prof. Shimshon Belkin, Hebrew University of

Jerusalem, Israel. *E. coli* strains used in this study are presented in [Table 2](#).

Table 2. *E. coli* biosensor strains used in this study.

<i>E. coli</i> RFM443	<i>GrpE</i>	<i>Lux</i>	Protein damage and general toxicity	Bae et al., (2020) ; Matejczyk et al., (2023)
<i>E. coli</i> RFM443	<i>LacZ</i>	<i>Lux</i>	General toxicity	Bae et al., (2020) ; Matejczyk et al., (2023)
<i>E. coli</i> RFM443	<i>RecA</i>	<i>Lux</i>	Genotoxicity	Melamed et al., (2012) , Matejczyk et al., 2020a , Matejczyk et al., 2020b , Matejczyk et al., 2020c , Matejczyk et al., 2022 , Matejczyk et al., 2023

2.3. Test on antimicrobial effects

Antimicrobial activity of VA, *iso*-VA and *orto*-VA was determined based on the growth inhibition effect of *E. coli*, *Sarcina* spp., *E. homaechei*, *S. aureus*, and *C. albicans*. Strains were cultured overnight at 37°C on Luria Bertani broth (LB) that contained casein peptone 10 g/L, yeast extract 5 g/L, NaCl 10 g/L, pH 7.0. Then, the overnight cultures were diluted 10-fold in fresh LB broth, and they were incubated at 37°C with shaking (130 rpm) to reach the log phase (OD₆₀₀=0.2). VA, *iso*-VA and *orto*-VA were added in the appropriate concentration (0.01, 0.1; 1, 10 and 100 mg/L) to the culture of microorganisms and incubated at 37°C for 24 and 48 h. The control sample did not contain the tested chemical compounds. The toxic effect of tested chemicals was measured with Optical Density (OD) at 600 nm using a GloMax® microplate reader (Promega, MA, USA). The antimicrobial activity of VA, *iso*-VA, and *orto*-VA was presented as an inhibition or stimulation of bacterial/fungal culture growth after 24 and 48 h, compared to the control cells and presented as a percentage (%). Experiments were conducted in triplicate.

2.4. Toxicity and protein damage determination

Two bacterial biosensor strains, *E. coli* RFM443, with plasmid transcriptional fusion of *grpE* and *lac* promoters with *luxCDABE* gene, were used to determine toxicity and degree of cellular protein damage. In this biosensor, a series of biochemical reactions with enzyme-luciferase participation leads to bioluminescence formation ([Bae et al., 2020](#)). The promoter – *grpE* in *E. coli* *grpE:luxCDABE* belongs to the group of inducible promoters, which are sensitive to general toxicity and protein damage ([Bae et al., 2020](#)). GrpE protein plays an important role in the protein folding process and the cellular heat shock response. The bioluminescent signal generated by *E. coli*

grpE:lucCDABE bacterial cells is proportional to the toxic effect and the degree of protein degradation after exposing the bacteria to VA, *iso*-VA and *orto*-VA at the concentrations of 0.01, 0.1, 1, 10 and 100 mg/L. In the second bioluminescence, *E. coli* RFM443 *lac:lucCDABE* plasmid with *lac* promoter signal is generated constitutively. In this strain, the toxic effect of tested chemical compounds was proportional to the decrease in luminescence. In this experiment, after the overnight cultivation of both bacteria strains in Luria Bertani (LB) medium with 100 µg/ml of ampicillin at 37°C, cultures were diluted in fresh LB and regrown at 37°C with shaking (150 rpm) to the early log phase (OD600=0.2). The measurements were carried out in white plates. To each well of the 96-well plate with an optical bottom (Grainer Bio-One, Germany), the volumes of 100 µl of appropriate concentrations of VA, *iso*-VA and *orto*-VA and 100 µl of *E. coli* RFM443 *grpE:lucCDABE* and *E. coli* RFM443 *lac:lucCDABE* cultures were added. The plates were incubated at 37°C for 2 and 24 hours, and luminescence was measured using a GloMax® microplate reader (Promega, MA, USA). Moreover, to normalize the luminescence value to the bacterial concentration, the OD600 was measured spectrophotometrically. The toxic and protein damage effects were presented as a percentage (%) increase/decrease in luminescence of treated samples compared to the control. The experiment was carried out in three independent series.

2.5. VA, *iso*-VA and *orto*-VA genotoxicity determination

Over the last quarter of a century, microbial biosensors containing *lux* (luminescence method) or *gfp* (green fluorescent protein) (fluorescence method) reporter genes have been used in environmental monitoring of metals in contaminated soils, polychlorinated biphenyls (PCBs) in wastewaters, organic pollutants in treated wastewaters, chromium, arsenic, lead, pesticides and petroleum hydrocarbons in waters, quorum sensing phenomena and microbial communities in soils (Moraskie et al., 2021, Zhu et al., 2022). So far, microorganisms, including *E. coli* strains containing the *recA:lucCDABE* plasmid gene construct, have been used to determine the genotoxicity of many chemical compounds, including antibiotics (Melamed et al., 2012), phenol, chromium (Cr⁶⁺), lead (Pb²⁺) and radiation potential. UV on bacterial cells (Jiang et al., 2017). In environmental monitoring, *E. coli* *recA:lucCDABE* strains were used to determine the genotoxicity of crude oil in surface water samples and the genotoxicity of municipal wastewaters (Moraskie et al., 2021, Zhu et al., 2022, Rojas-Villacorta et al., 2022a, Rojas-Villacorta et al., 2022b). In the work of Zappi et al. (2021), microbiological *E. coli* biosensors containing the *lux* and *gfp* gene were used to determine the toxic impact of nitrification inhibitors (allylthiourea, phenol and copper) in industrial and municipal wastewaters.

The *E. coli* RFM443 *recA:lucCDABE* bacterial biosensor with a plasmid gene construct

and a fusion of the *recA* promoter with the *luxCDABE* reporter gene was used to determine the genotoxicity of VA, *iso*-VA and *orto*-VA at the concentration of 0.01; 0.1; 1, 10 and 100 mg/L. The *recA* promoter belongs to the group of DNA damage-induced gene promoters involved in the SOS repair system. *E. coli* strain *recA:luxCDABE* was cultured for 24 hours in LB broth with ampicillin at a 100 µg/ml concentration at 37°C. After a 24-hour incubation, the culture was diluted in fresh LB broth with ampicillin at a concentration of 100 µg/ml and incubated at 37°C with shaking (150 rpm) until a logarithmic growth phase of OD₆₀₀=0.2 was reached. The appropriate solutions of VA, *iso*-VA and *orto*-VA were added to the LB broth cultures of *E. coli recA:luxCDABE* and incubated for 2 and 24 hours at 37°C. To standardize the luminescence response of the *E. coli recA:luxCDABE* culture for all test samples and the control samples, the OD at 600 nm was spectrophotometrically determined. A GloMax® microplate reader (Promega, MA, USA) was used to measure luminescence and absorbance. Luminescence measurement and data analysis were performed according to the method described by [Melamed et al. \(2012\)](#) and [Kessler et al. \(2012\)](#). Luminescence was measured for all tested and control samples. The dynamic of the induction of *recA* promoter after 2 and 24 hours incubation of *E. coli recA:luxCDABE* cultures with the test chemicals was presented as the percentage (%) increase/decrease in luminescence compared to the control sample. The experiment was performed in triplicate.

2.6. ROS generation

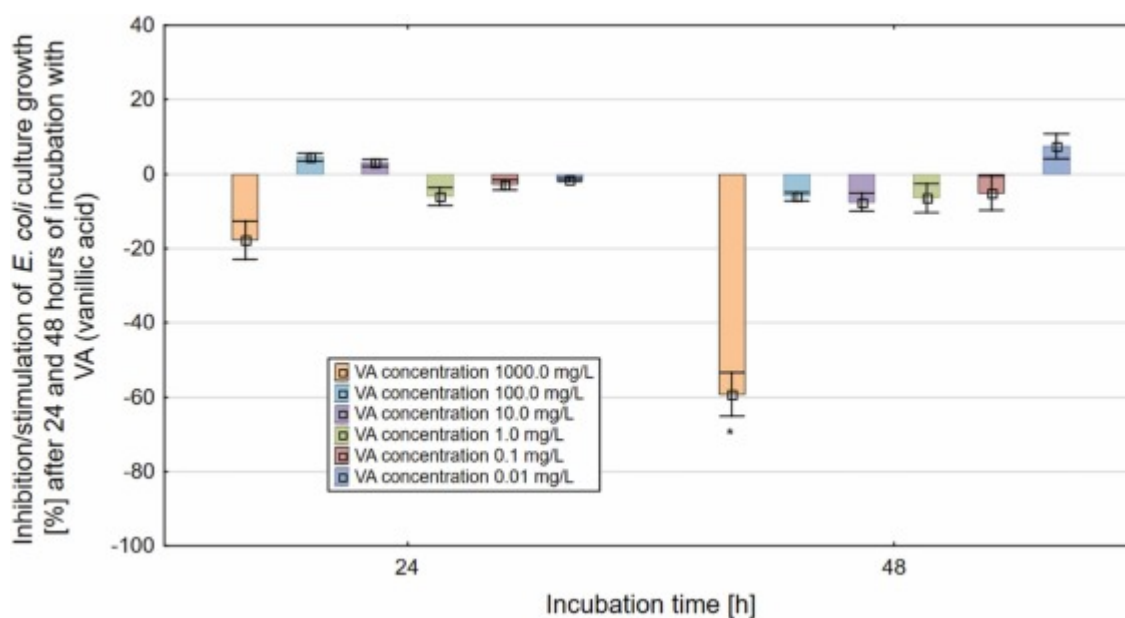
The ROS synthesis in *E. coli* ATCC-25922 after treatment with VA, *iso*-VA and *orto*-VA at the concentration of 0.01, 0.1, 1, 10 and 100 mg/L was determined using 7'-dichlorofluoresceindiacetate (DCFH-DA) (Sigma-Aldrich, UK), according to the method described by [Matejczyk et al., 2020a](#), [Matejczyk et al., 2020b](#), [Matejczyk et al., 2020c](#). The overnight culture of *E. coli* in LB broth at 37°C was diluted in fresh LB broth and then incubated at 37°C with shaking (130 rpm) to reach the log phase (OD₆₀₀ =0.2). The *E. coli* culture was treated with VA, *iso*-VA, and *orto*-VA at concentrations of 0.01, 0.1, 1, 10 and 100 mg/L. Next, DCFH-DA was added to each sample at a final concentration of 5 µM and incubated at 37°C for 45 min. As the control, non-treated bacterial suspensions were used. The DCF fluorescence intensity was measured using GloMax® microplate reader (Promega, MA, USA) at the excitation wavelength of 485 nm and the emission wavelength of 535 nm. In this method, the fluorescence intensity of the treated sample is proportional to the degree of ROS generation. At the same time, for each sample, the OD₆₀₀ values of bacteria cultures were monitored spectrophotometrically. The ROS generation in *E. coli* culture treated by VA, *iso*-VA and *orto*-VA was presented as a percent (%) of ROS increase compared to the not treated control culture. All the experiments were performed in triplicates.

2.7. Statistical analysis

For statistical analysis, the Tukey test was used. This test was chosen because of the existence of a normal distribution for the individual variables included in the study according to the Shapiro-Wilk test results and the heterogeneity of variance according to the Bartlett test. Statistical calculations were done using Statistica 13.1 (TIBCO, Software, Inc.). Significant differences were taken as $\alpha = 0.05$.

3. Results

The complete set of results regarding antimicrobial activity, toxicity, degree of degradation of cellular proteins, genotoxicity and generation of oxidative stress of VA and its isomers *iso*-VA and *orto*-VA are presented in Fig. 1-27 and [Supplementary materials](#) (S1-S13).



[Download: Download high-res image \(152KB\)](#)

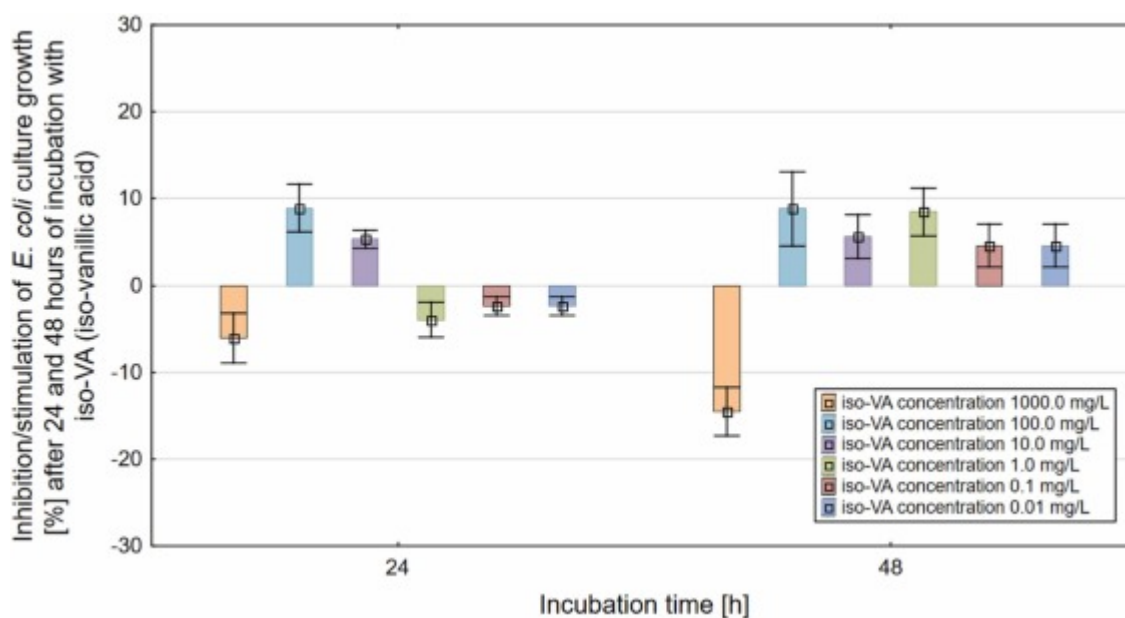
[Download: Download full-size image](#)

Fig. 1. The antimicrobial activity of VA against *E. coli* ATCC-25922. * - statistically significant difference at $\alpha = 0.05$ between control sample. Error bars indicate the standard deviation (SD) of the mean of three independent replicates.

3.1. Antimicrobial activity of VA, *iso*-VA, and *orto*-VA

Our finding demonstrated that VA, *iso*-VA, and *orto*-VA exhibited varying effects on the growth of *E. coli* ATCC-25922, *Sarcina* spp. ATCC-35659, *E. homaechei* LBM ATCC-700323, *S. aureus* ATCC-25923 and *C. albicans* ATCC-10231 across different concentrations (Fig. 1, [fig. 2](#), [fig. 3](#)). Specifically, after 24 h, significant *E. coli* culture growth stimulation was observed for *orto*-VA at 100 mg/L (10.4%) and 0.01 mg/L

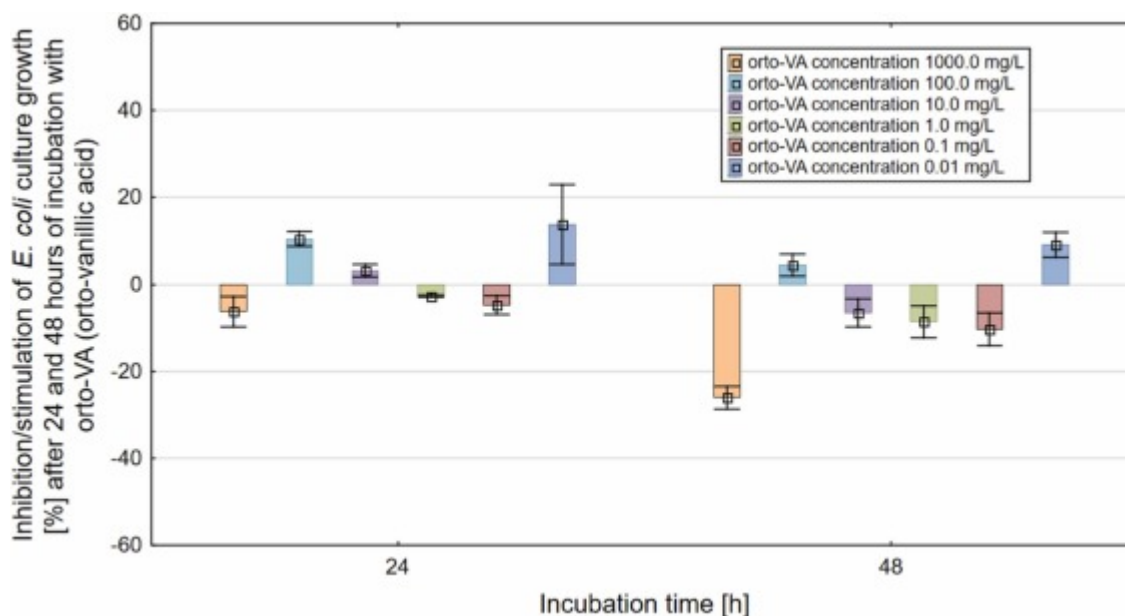
(13.7%) concentrations. Conversely, notable inhibition of *E. coli* growth was detected after 24 hours and 48 hours, with a 17.8% and 59.3% reduction, respectively, at a concentration of 1000 mg/L VA and a 26.06% reduction after 48 hours at a concentration of 1000 mg/L *orto*-VA. The most pronounced stimulation of *Sarcina* spp. growth (10.5%) occurred after 24 hours at concentrations of 10 mg/L for both *iso*-VA and *ortho*-VA. Conversely, the most significant increase in the inhibition of bacteria growth for *Sarcina* spp. was noted after 24 hours (83.8%, 69.6%, and 69.9%, respectively) and 48 hours (80.3%, 70.8%, and 65.1%, respectively) After 48 hours, the most pronounced stimulation of bacteria growth, at 16.7%, was observed with a concentration of 0.01 mg/L for *iso*-VA. After 48 h, the greatest enhancement of the toxic effect of VA and *orto*-VA (28.4% and 26.4%, respectively) for *E. homaechei* culture development in the concentration of 1000 mg/L was observed. Both after 24 h and after 48 h, the inhibition effect of VA and *orto*-VA for *S. aureus* ATCC-25923 growth was found. The most significant inhibition of the growth of *S. aureus* culture was observed after 24 h in the concentrations of 100 mg/L and 10 mg/L *orto*-VA (36.8% and 30.7%, respectively). However, the maximum inhibition of the growth of *C. albicans* ATCC-10231 culture was found after 24 h and 48 h in a dose of 100 mg/L VA (35.9%, 33.4%, respectively) and after 48 h in a dose of VA 1000 mg/L (31.8%). In turn, after 24 h in the concentrations of 100, 10, 1, 0.1 and 0.01 mg/L *iso*-VA, the stimulating effect for *C. albicans* growth in the range of 2.03% (0.01 mg/L) to 11.6% (100 mg/L) was observed.



Download: [Download high-res image \(158KB\)](#)

Download: [Download full-size image](#)

Fig. 2. The antimicrobial activity of *iso*-VA against *E. coli* ATCC-25922. * - statistically significant difference at $\alpha = 0.05$ between control sample. Error bars indicate the standard deviation (SD) of the mean of three independent replicates.



[Download: Download high-res image \(157KB\)](#)

[Download: Download full-size image](#)

Fig. 3. The antimicrobial activity of *orto*-VA against *E. coli* ATCC-25922. * - statistically significant difference at $\alpha=0.05$ between control sample. Error bars indicate the standard deviation (SD) of the mean of three independent replicates.

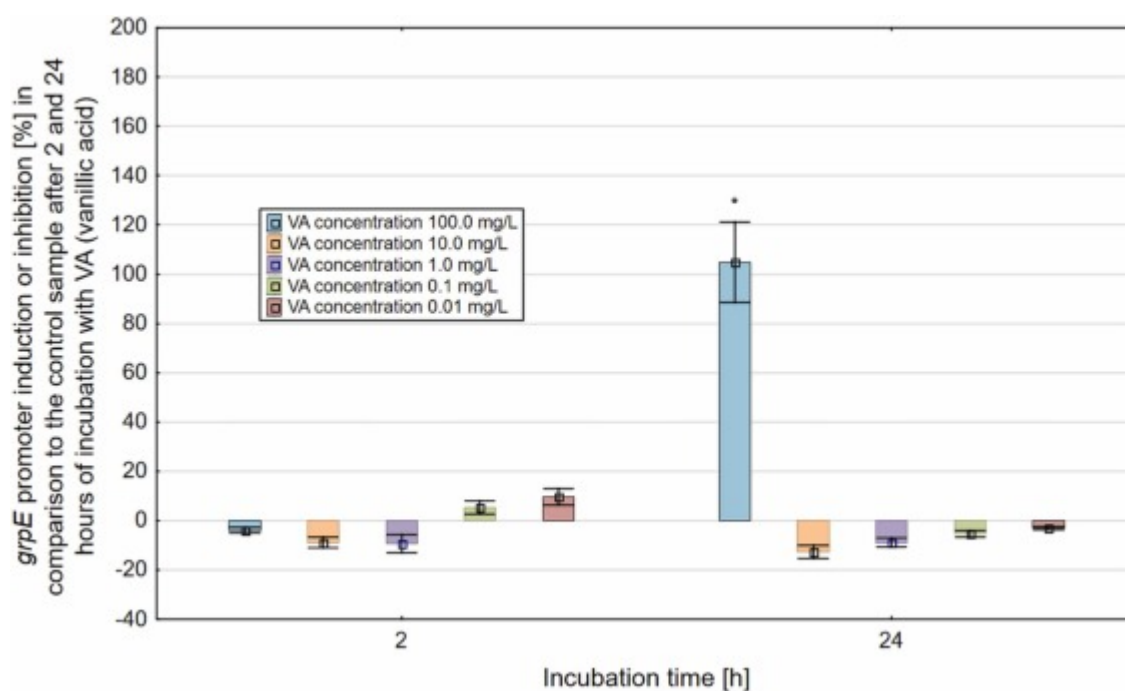
3.2. Significant differences in VA, *iso*-VA and *orto*-VA antimicrobial activity

Significant differences in the antimicrobial activity of VA, *iso*-VA, and *orto*-VA are presented in [Figures S1–S13](#). A significant difference ($\alpha=0.05$) in the growth inhibition of *E. coli* after treatment with VA was noticed only for a concentration of 1000.0 mg/L after 48 hours ([Figure S1](#)). Conversely, significant differences ($\alpha=0.05$) in growth inhibition of *Sarcina* spp. were observed between control and treatment groups after 24 and 48 hours of incubation across various doses of VA (1000.0, 100.0, and 10.0 mg/L), as well as for *iso*-VA and *orto*-VA at 1000.0 mg/L ([Figures S1, S6, S10](#)). For *E. homaechei*, statistically significant differences ($\alpha=0.05$) in growth inhibition by *iso*-VA were observed at a dose of 1000.0 mg/L compared to the control group after 48 hours of incubation ([Figures S3, S7, S11](#)). No statistically significant differences were noted for *S. aureus* following VA treatment ([Figure S4, S8, S12](#)). However, significant differences ($\alpha=0.05$) in growth inhibition were observed for *iso*-VA at doses of 1.0, 0.1, and 0.01 mg/L after 48 hours of incubation ([Figure S8](#)), while *orto*-VA showed significant differences at doses of 1000.0 and 100.0 mg/L after 24 hours of incubation compared to the control group.

3.3. Determination of the VA, *iso*-VA and *orto*-VA toxicity and the

potential for protein damage

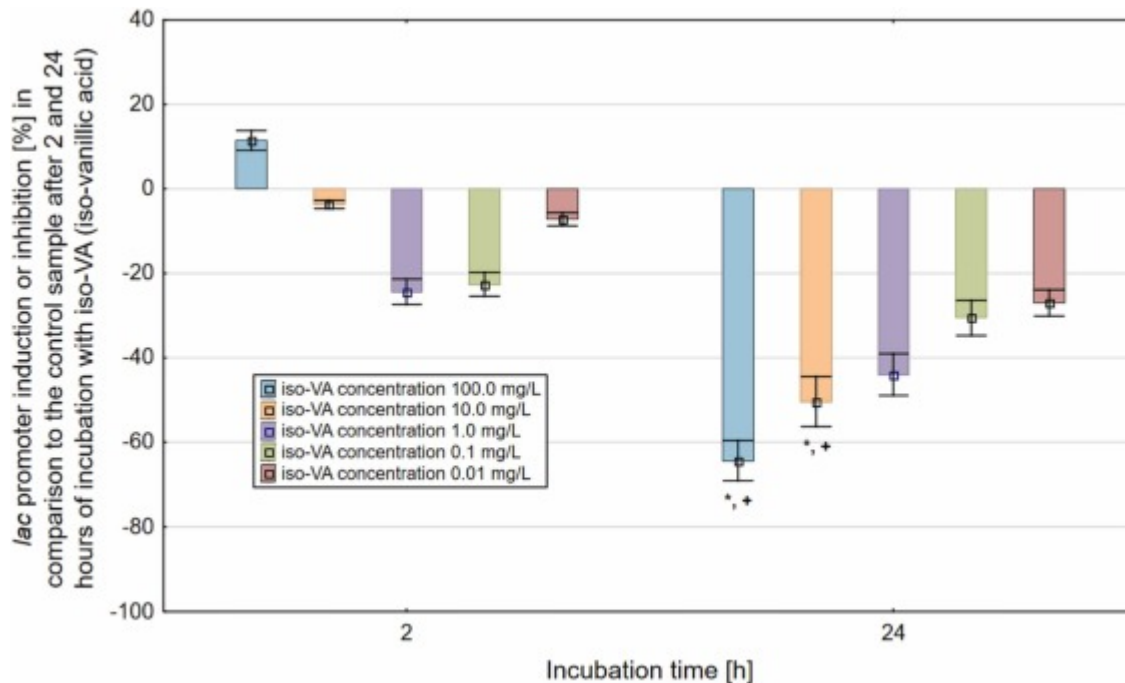
To assess the toxicity and protein degradation potential of VA, *iso*-VA, and *orto*-VA, we utilized two distinct bioluminescent *E. coli* biosensor strains, *E. coli* RFM 443 *grpE:lucCDABE* and *E. coli* RFM443 *lac:lucCDABE*. Our finding showed that after 24 h of exposure, VA, *iso*-VA, and *orto*-VA at a dose of 100 mg/L significantly induced the *grpE* promoter and led to increased bioluminescence synthesis in *E. coli* RFM 443 *grpE:lucCDABE* cells (104.8%, 136.8%, and 141.9%, respectively) (Fig. 4). In addition, the stimulating effect of *iso*-VA at low doses of 0.1 mg/L (9.86%) and 0.01 mg/L (18.9%) on *grpE* promoter induction has also been observed. However, the reduction of *grpE* promoter activity and bioluminescence decrease in *E. coli* RFM 443 *grpE:lucCDABE* were detected after 2 h and 24 h of bacteria treatment with VA, *iso*-VA and *orto*-VA. The most significant toxic and protein degradation effects were found after 24 h in 1 mg/L *iso*-VA (27.86%) and 10 mg/L *orto*-VA (42.9%) doses. A pronounced inhibitory effect on *E. coli lac:lucCDABE* bioluminescence was evident upon exposure to VA, *iso*-VA, and *orto*-VA. Specifically, VA induced a substantial reduction in bacteria bioluminescence, with the most notable decreases (72.53% and 69.86%) observed after 24 hours at doses of 10 mg/L and 100 mg/L, respectively. Similarly, both *iso*-VA and *orto*-VA at doses of 10 and 100 mg/L significantly suppressed the bioluminescence signal (ranging from 50.36% to 64.36% and 59.62–43.23%, respectively) in the *E. coli lac:lucCDABE* strain (Fig. 5). Conversely, after 2 hours of treatment with VA (100 mg/L), a significant stimulating effect on bioluminescence synthesis (up to 36.6%) in bacterial cells was observed.



Download: [Download high-res image \(166KB\)](#)

Download: [Download full-size image](#)

Fig. 4. Effect of studied doses of VA on *grpE* promoter response in *E. coli* RFM443 *grpE:lucCDABE* (toxicity and protein damage), presented as a percent (%) of the induction or inhibition. * - statistically significant difference at $\alpha = 0.05$ between control sample. Error bars indicate the standard deviation (SD) of the mean of three independent replicates.



[Download: Download high-res image \(167KB\)](#)

[Download: Download full-size image](#)

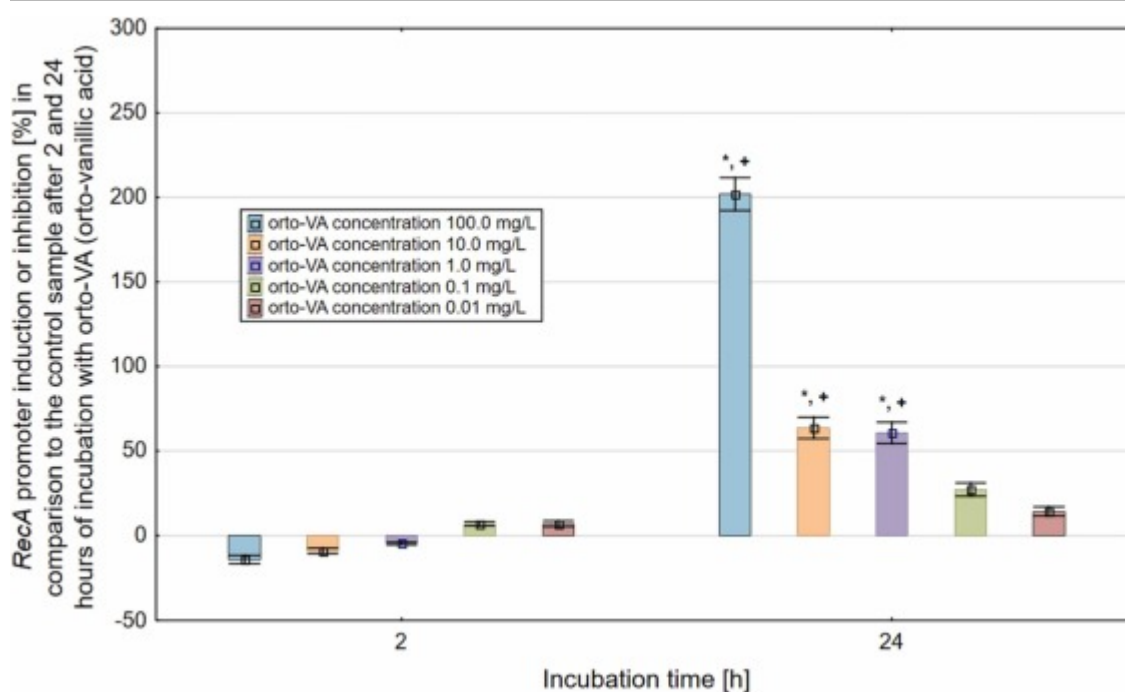
Fig. 5. Effect of studied doses of *iso*-VA on *lac* promoter response in *E. coli* RFM443 *lac:lucCDABE* (toxicity), presented as a percent (%) of the induction or inhibition. * - statistically significant difference at $\alpha = 0.05$ between control sample. + - statistically significant difference at $\alpha = 0.05$ between sample after 2 h. Error bars indicate the standard deviation (SD) of the mean of three independent replicates.

Our study showed significant toxicity and protein degradation potential of VA, *iso*-VA, and *orto*-VA in *E. coli* *grpE:lucCDABE* cells after 24 hours at a concentration of 100 mg/L. Among them, *orto*-VA exhibited the highest toxicity, with a value of 141.9%. Notably, *iso*-VA and *orto*-VA displayed higher toxicity and protein degradation than VA, with values of 136.8% for *iso*-VA and 141.9% for *orto*-VA, while VA showed 104.8%. However, there were no significant differences in toxicity between *iso*-VA and *orto*-VA in *E. coli* *grpE:lucCDABE* cells. Additionally, significant toxicity of VA, *iso*-VA, and *orto*-VA on *E. coli* *lac:lucCDABE* was observed after 24 hours across all tested doses (0.01, 0.1, 1, 10, and 100 mg/L), with the highest value recorded for VA (72.5%) at a dose of 10 mg/L. The most substantial differences in toxicity values were observed between VA (44.8% at 1 mg/L) and *iso*-VA (44% at 1 mg/L), and *orto*-VA (14.06%), particularly at lower acid

concentrations (0.01, 0.1, and 1 mg/L).

3.4. VA, iso-VA and orto-VA genotoxicity estimation

The genotoxicity of VA, iso-VA, and orto-VA was evaluated based on the induction of the genotoxin-sensitive *recA* promoter, which was transcriptionally fused with the *luxCDABE* reporter gene in the *E. coli recA:luxCDABE* biosensor strain. The genotoxic effects of the tested compounds were assessed by measuring the induction of the *recA* promoter and the subsequent generation of bioluminescent signals in *E. coli recA:luxCDABE* cultures. After 24 hours, all tested doses of VA, iso-VA, and orto-VA induced the *recA* promoter, with maximum stimulation observed at a concentration of 100 mg/L for each compound (128.1% for VA, 637.74% for iso-VA, and 201.86% for orto-VA) (Fig. 6). Furthermore, iso-VA exhibited a significant increase in *recA* promoter activity and bioluminescence synthesis at doses of 10, 1, 0.1, and 0.01 mg/L, with values ranging from 113.26% to 132.06%. Interestingly, after 2 hours at the highest tested doses (1, 10, and 100 mg/L) of VA, iso-VA, and orto-VA, a slight inhibition of *recA* promoter activity and a decrease in bioluminescence generation were observed, with a maximum inhibition of approximately 15.6%.



Download: [Download high-res image \(165KB\)](#)

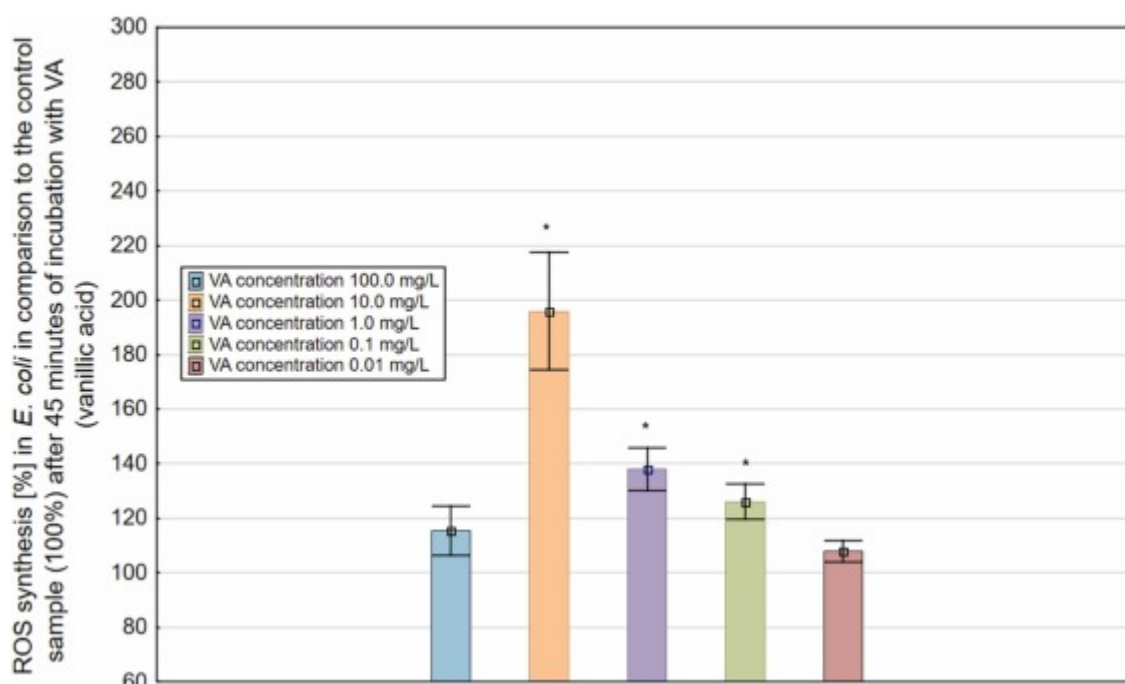
Download: [Download full-size image](#)

Fig. 6. Effect of studied doses of orto-VA on *recA* promoter induction in *E. coli* RFM443 *recA:luxCDABE* (genotoxicity), presented as a percent (%) of the induction. * - statistically significant difference at $\alpha = 0.05$ between control sample. + - statistically significant difference at $\alpha = 0.05$ between sample after 2 h. Error bars indicate the standard deviation (SD) of the mean of three independent replicates.

Fig. 6.

3.5. ROS synthesis

In the culture of *E. coli* ATCC-25922, a significant stimulating effect on ROS generation was observed for VA at a dose of 10 mg/L, increasing by 195.9% (Fig. 7). In comparison, *orto*-VA at 100 mg/L exhibited a stimulation of 166.85%. Moreover, in *E. coli* cells, both concentrations of *iso*-VA, 100 and 10 mg/L, significantly elevated ROS synthesis levels, reaching up to 139.13% and 143.26%, respectively. Additionally, *iso*-VA at a dose of 10 mg/L induced growth in ROS synthesis of up to 129.06%. Among the tested compounds, the highest induction of ROS synthesis in *E. coli* culture was observed for VA, with a maximum value of 138.01% at a dose of 1 mg/L.



Download: [Download high-res image \(161KB\)](#)

Download: [Download full-size image](#)

Fig. 7. Effect of studied doses of VA on ROS synthesis in *E. coli* ATCC-25922, presented as a percent (%) of the induction. * - statistically significant difference at $\alpha=0.05$ between control sample. Error bars indicate the standard deviation (SD) of the mean of three independent replicates.

3.6. Significant differences in toxicity, protein degradation, genotoxicity, and ROS synthesis

For the effect of VA on the *grpE* promoter in *E. coli* RFM443 *grpE:luxCDABE* (toxicity and cellular protein damage), statistically significant differences ($\alpha=0.05$) were observed at a dose of 100.0 mg/L VA after 24 h incubation. This difference manifested

as a marked increase in the induction of the *grpE* promoter after 2 hours of incubation (Figures S16–S18). For the changes in *lac* promoter (*E. coli* RFM443 *lac:lucCDABE*) induction, statistically significant differences ($\alpha=0.05$) were noticed for 100 mg/L of VA after the 2 h incubation (Figures S14–S19). Statistically significant differences ($\alpha=0.05$) were observed for all tested acids (VA, *iso*-VA and *orto*-VA) compared to the control group after 2 and 24 h incubation at doses of 100.0 and 10.0 mg/L. In the first case, the statistically significant difference concerned the induction of *lac* promoter after 2 h incubation ($\alpha=0.05$), while the second case described the inhibition of *lac* promoter after 24 h incubation ($\alpha=0.05$). Regarding the effect of the individual acids on the change in *recA* promoter induction (*E. coli* RFM443 *recA:lucCDABE*), diverse patterns were observed depending on the type of acid and its dose (Figures S20–S22). Statistically significant differences ($\alpha=0.05$) were noticed between the control after 2 h incubation and the *recA* promoter induction after 24 h incubation with VA and *iso*-VA. These differences were associated with the increased induction of the *recA* promoter, observed for both VA and *iso*-VA across all tested concentrations. In the case of *orto*-VA, a significant difference was noticed compared to the control after 2 h of incubation at a dose of 100 mg/L. Regarding ROS generation (Figures S23–S25), statistically significant differences ($\alpha=0.05$) were observed between the control and VA at 10.0, 1.0, and 0.1 mg/L doses. For *iso*-VA, statistically significant differences ($\alpha=0.05$) were observed at doses of 100.0, 10.0, and 1.0 mg/L, while for *orto*-VA, statistically significant differences ($\alpha=0.05$) were noticed at doses of 100.0, 10.0, 1.0, and 0.1 mg/L.

4. Discussion

The objective of this study was to conduct a comparative analysis of the antimicrobial effects, toxicity, genotoxicity, and oxidative stress-inducing capabilities of VA in relation to its *iso*-VA and *orto*-VA isomers. This research represents the first reported attempt to compare the biological properties of VA with *iso*-VA and *orto*-VA isomers. The results observed in this investigation provide compelling evidence that VA and its isomers exhibit antimicrobial activity against the bacterial strains tested. The antimicrobial properties of VA against bacterial pathogens have been reported in several studies. For example, Mourtzinis et al. (2009) observed growth inhibition of *S. aureus* and *E. coli* cultures after exposure to the VA. However, Qian et al. (2019) documented the antibacterial properties of VA against *E. cloacae*. Additionally, Alves et al. (2013) elucidated the toxic effects of VA on *Pasteurella multocida*, and *Neisseria gonorrhoeae*. Existing literature indicates that VA can disrupt the biofilm formation of clinical pathogens by inhibiting quorum sensing (QS) signalling mechanisms (Caetano et al., 2023, Duskaev et al., 2023). The antimicrobial properties

of VA are not fully understood, but it is suggested that its antimicrobial activity may be correlated with the destabilization of microbial cell surfaces and cytoplasmic membranes (Girawale et al., 2022, Muddahally et al., 2023, Sha et al., 2023). Qian et al. (2019) observed a decrease in intracellular ATP concentration in carbapenem-resistant *E. cloacae* (CREC) upon treatment with VA, indicating disturbances in intracellular and extracellular ATP balance, which can lead to cell wall damage and disruption of intracellular structures. Additionally, disruption of cell membrane integrity by VA may result in the formation of pores and leakage of intracellular components into the extracellular space (Trombetta et al., 2005, Gill and Holley, 2006, Qian et al., 2019, Duskaev et al., 2023).

Our finding revealed distinct antimicrobial activity profiles of *iso*-VA and *orto*-VA, compared to VA across tested bacterial strains. Specifically, *orto*-VA exhibited a more pronounced antimicrobial effect than *iso*-VA at 100 mg/L and 1000 mg/L concentrations, which can suggest that the VA isomerism and related differences in the chemical structure of *iso*-VA and *orto*-VA affect the antimicrobial efficacy of VA isomers. Although the antimicrobial activity of VA has been extensively studied ((Girawale et al., 2022; Muddahally et al., 2023; Sha et al., 2023), there is a lack of research focusing on the antimicrobial properties of *iso*-VA and *orto*-VA isomers. Therefore, the results presented in our study provide new insight into the biological activity of VA isomers. Previous reports have highlighted that phenolic compounds, upon cell wall destruction and intracellular penetration, can interact with various intracellular components, including proteins (Trombetta et al., 2005, Lou et al., 2011, Duskaev et al., 2023). Consequently, the distinct chemical structures of VA, *iso*-VA, and *orto*-VA may influence the efficiency and nature of interactions between these compounds and cellular components, potentially modulating their antimicrobial activity. Nonetheless, further research is warranted to elucidate the mechanisms underlying the differential antimicrobial effects of VA, *iso*-VA, and *orto*-VA.

On the other hand, the stimulating effect of VA, *iso*-VA, and *orto*-VA on bacterial growth at doses ranging from 100 mg/L to 0.01 mg/L observed in our study may be attributed to their antioxidant properties. Previous studies have reported that the phenolic structure of VA determines its antioxidant activity (Kaur et al., 2022, Muddahally et al., 2023). Phenolic compounds have been shown to act as indirect modulators of intracellular pro- and anti-oxidant enzymes (Kyselova, 2011). It has been reported that VA can enhance the antioxidant status of cells by increasing the activation of enzymes such as glutathione peroxidase, superoxide dismutase, and catalase (Christaki et al., 2012, Maqsood et al., 2014), as well as scavenging free radicals and reducing ROS production (Kaur et al., 2022, Muddahally et al., 2023).

In our study, to evaluate the toxicity, protein damage, and genotoxicity of VA and its isomers, three distinct bioluminescent *E. coli* biosensor strains were utilized. Microbial biosensors containing *lux* (luminescence method) or *gfp* (green fluorescent protein) (fluorescence method) reporter genes have been used in environmental monitoring of metals in contaminated soils, polychlorinated biphenyls (PCBs) in wastewaters, organic pollutants in treated wastewaters, chromium, arsenic, lead, pesticides and petroleum hydrocarbons in waters, quorum sensing phenomena and microbial communities in soils (Moraskie et al., 2021, Zhu et al., 2022). So far, microorganisms, including *E. coli* strains containing the *recA:luxCDABE* plasmid gene construct, have been used to determine the genotoxicity of many chemical compounds (Melamed et al., 2012, Jiang et al., 2017). In environmental monitoring, *E. coli recA:luxCDABE* strains were used to determine the genotoxicity of crude oil in surface water samples and the genotoxicity of municipal wastewaters (Moraskie et al., 2021, Zhu et al., 2022, Rojas-Villacorta et al., 2022a, Rojas-Villacorta et al., 2022b). Zappi et al. (2021) utilized *E. coli* biosensors containing the *lux* and *gfp* genes to determine the toxic impact of nitrification inhibitors (allylthiourea, phenol and copper) in industrial and municipal wastewaters. Similarly, *lux*-based *E. coli* strains have been used in the design of biosensors to study the toxicity and genotoxicity of various chemical compounds such as antibiotics, non-steroidal anti-inflammatory drugs (NSAIDs), 17 β -estradiol, natural compounds such as caffeic, rosmarinic and mandelic acids and its metal complexes (Bae et al., 2020, Ali et al., 2021, Moraskie et al., 2021, Zhu et al., 2022, Rojas-Villacorta et al., 2022a, Rojas-Villacorta et al., 2022b, Matejczyk et al., 2022).

In this study, VA, *iso*-VA and *orto*-VA after 24 h in dose of 100 mg/L showed significant toxicity and protein degradation potential with a maximum value for *orto*-VA using *E. coli grpE:luxCDABE*. The *iso*-VA and *orto*-VA were characterized by higher toxicity and degree of protein degradation compared to VA; however, between *iso*-VA and *orto*-VA, there were no significant differences in the toxic effect on *E. coli grpE:luxCDABE* cells. The phenolic structure of VA and its isomers can be linked with their genotoxicity via disruption of the intracellular receptor functions and binding to the genomic DNA in bacteria cells (Duskaev et al., 2023). The results also showed that VA, *iso*-VA and *orto*-VA at a dose of 10 mg/L were highly toxic for *E. coli lac:luxCDABE* strain after 24 h of incubation. Moreover, a similar effect was observed for *E. coli recA:luxCDABE* strain. As mentioned earlier, the toxicity mechanism of phenolic acids, including VA, is mainly related to their ability to destabilize and damage the bacterial cell wall and various intracellular organelles. Cellular disorders associated with the leakage of intracellular components lead to dysregulation of the functionality of proteins and cell death (Qian et al., 2019, Duskaev et al., 2023).

In living cells, the imbalance between the synthesis of oxygen-reactive species (ROS) and the detoxification of these reactive products leads to oxidative stress (Islas-Flores et al., 2017, Pizzino et al., 2017). ROS include superoxide radicals ($O_2^{\bullet-}$), hydrogen peroxide (H_2O_2), hydroxyl radicals ($\bullet OH$), and singlet oxygen (1O_2) (Hajam et al., 2022; Sazykin et al., 2023). Increased ROS levels cause serious damage to crucial cellular structures like proteins, lipids, and nucleic acids (Schieber et al., 2014; Muddahally et al., 2023). RNA, compared to DNA, is more sensitive to ROS. RNA in the cell is the primary regulator of gene expression. RNA constitutes 80–90% of the total cellular nucleic acids in bacterial cells. The main RNA damages caused by ROS include the formation of abasic sites, strand breaks or modifications of base and sugar moieties (Seixas et al., 2022, Buchser et al., 2023). In the last decade, apart from studies on the antioxidant potential of phenolic compounds, including phenolic acids, flavonoids, or curcuminoids, the number of studies describing their pro-oxidative and apoptosis-inducing properties has also increased. It is known that the pro-oxidant activity of these chemical compounds is correlated with the ability to generate oxidative stress in cells. In turn, apoptosis as programmed cell death is necessary to maintain a proper balance between cell proliferation and cell death, and disturbances of this balance lead to cancer growth (Kashyap et al., 2021). The primary mechanism of pro-oxidative activity of phenolic compounds is the ability to interact with transition metals commonly found in biological systems of the cell (Rahman et al., 2022). Several reports suggest that the pro-oxidant action of plant-derived phenolics rather than their antioxidant action may be a key mechanism of their toxicity and anticancer potential (Kyselova, (2011); Rahman et al. (2022).

In our study, we analysed reactive oxygen species (ROS) production in *E. coli* cultures to quantify the level of oxidative stress induced by exposure to the tested chemical compounds. We observed a significant increase in the oxidative stress in *E. coli* by increasing ROS production after VA, *iso*-VA, and *orto*-VA exposure; the most significant increase in ROS generation was found for VA (10 mg/L) and *orto*-VA (100 mg/L). We suppose that the toxicity of VA, *iso*-VA, and *orto*-VA in *E. coli* strains may be attributed to their pro-oxidative potential. Moreover, in all of the tested concentrations, after 24 h, especially for *iso*-VA and *orto*-VA, high genotoxic activity was detected in the *E. coli recA:luxCDABE* strain. The observed increased free radicals level after *E. coli recA:luxCDABE* exposition to VA, *iso*-VA and *orto*-VA could be associated with bacterial DNA damage. Consequently, ROS may stimulate the induction of the *recA* promoter as an indicator of genotoxicity (Hajam et al., 2022, Rahman et al., 2022).

The toxicity of VA using the *E. coli* RFM443 *lac:luxCDABE* was significantly different compared to the toxicity of VA and *iso*-VA, mainly at concentrations of 100, 1, 0.1 and

0.01 mg/L After 24 h, the most significant differences were found in the genotoxicity of *iso*-VA compared to VA and *orto*-VA, in all tested concentrations. Also, the most significant differences were observed in the ROS generation values for VA compared to *iso*-VA and *orto*-VA, especially at concentrations of 100 and 10 mg/L.

Our study confirms that the isomerisms of various chemical compounds impact their biological activity (Lu and Gan, 2014, Tu et al., 2022). Differences in the arrangement of –OH and CH₃ groups in the aromatic ring in VA, *iso*-VA and *orto*-VA may affect their ability to interact with cellular components such as proteins or DNA, leading to differential toxic and genotoxic activities. To assess toxicity, degradation of cellular proteins and genotoxicity of tested chemicals, we employed an *E. coli* strain with a transcriptional fusion of the *grpE* and *lac* promoters with the *luxCDABE* reporter gene. Differences in the chemical structure of VA and its isomers could alter the nature of the interaction between the tested compounds and the *grpE* and *lac* promoter region, consequently affecting the expression level of the *luxCDABE*. Our findings align with those reported by Melamed et al. (2012), Bae et al. (2020), and Belkin and Cheng (2023), indicating that the level of induction of the *grpE* and *lac* promoters and the expression of the *luxCDABE* are dependent on the chemical structure of the tested compounds. Furthermore, compared to VA, *iso*-VA and *orto*-VA may impact the synthesis of chemiluminescence in *E. coli* cells and the emission intensity of the luminescent signal (Yin et al., 2022, Belkin and Cheng, 2023).

In summary, this comprehensive approach enabled us to discern potential differences in toxicity, genotoxicity, and oxidative stress induction among VA and its *iso*- and *ortho*-isomers, providing valuable insights into their safety profiles and biological activities.

5. Conclusions

The experiments outlined in this study concern basic investigations into the biological activities of VA and its isomeric forms, *iso*-VA and *orto*-VA. Currently, the research is shifting focus towards delving deeper into understanding the molecular mechanisms underlying the toxicity of the compounds under scrutiny. The elevated levels of reactive oxygen species (ROS) observed in our study suggest that oxidative stress is the primary mechanism driving the toxic and genotoxic impacts of VA and its isomers on bacterial cells. A more comprehensive analysis should explore additional parameters related to oxidative stress, such as cellular glutathione levels and the activities of antioxidant enzymes like superoxide dismutase, catalases, and peroxidases. Our findings demonstrate that VA and its *iso*- and *orto*-isomers exhibit toxic and genotoxic effects on the tested bacteria strains. Phenolic compounds,

including VA, commonly found in wastewater, possess toxicity that can negatively affect the microorganisms within activated sludge. This impairment may lead to compromised sludge functionality and reduced efficiency in biodegrading xenobiotics in sewage. Hence, it is imperative to continually seek and implement more productive wastewater treatment technologies for phenolic compounds. The results presented indicate that in addition to VA, its *iso*- and *orto*-isomers possess antimicrobial properties, suggesting their potential as candidates for food preservatives. However, further in-depth investigations on the biological activities of VA and its isomers, specifically regarding their suitability as food preservatives, are warranted. Moreover, establishing safe dosages of these compounds as food preservatives for human consumption is essential for practical application. Furthermore, obtained results indicated that *E. coli* strains with the plasmid-based genetic constructs *grpE:luxCDABE*, *lac:luxCDABE* and *recA:luxCDABE* are useful as microbial biosensors in the toxicity, protein degradation and genotoxicity estimation of VA and its isomers *iso*-VA and *orto*-VA.

Funding

This work was supported by the National Science Centre (NCN), Poland ([2020/39/B/NZ9/01894](#)).

CRediT authorship contribution statement

Włodzimierz Lewandowski: Visualization, Validation, Supervision. **Piotr Ofman:** Formal analysis, Data curation. **Marzena Matejczyk:** Writing – review & editing, Writing – original draft, Visualization, Validation, Supervision, Methodology, Investigation, Formal analysis, Data curation, Conceptualization. **Renata Świsłocka:** Visualization, Validation, Supervision, Conceptualization. **Edyta Juszczuk-Kubiak:** Visualization, Validation, Supervision, Formal analysis. **Kavindra Kumar Kesari:** Visualization, Validation, Supervision. **Wong Ling Shing:** Visualization, Validation, Supervision. **Balu Prakash:** Visualization, Validation, Supervision.

Declaration of Competing Interest

The authors declare that they have no known competing financial interests or personal relationships that could have appeared to influence the work reported in this paper.

Acknowledgements

Authors are very grateful to Professor Shimshon Belkin, Dr. Tal Elad, Dr. Liat Moscovici and Dr. Sharon Yagur-Kroll, Institute of Life Sciences, The Hebrew University of Jerusalem, Jerusalem, Israel for providing bacteria strains.

Appendix A. Supplementary material

 [Download: Download Word document \(1006KB\)](#)

Supplementary material.

[Recommended articles](#)

Data availability

Data will be made available on request.

References

[Ali et al., 2021](#) S.A. Ali, D. Mittal, G. Kaur

In situ monitoring of xenobiotics using genetically engineered whole cell based microbial biosensors: recent advances and outlook

World J. Microbiol. Biotechnol., 7 (2021), pp. 37-81, [10.1007/s11274-021-03024-3](#) ↗

[View in Scopus](#) ↗ [Google Scholar](#) ↗

[Alves et al., 2013](#) M.J. Alves, I.C. Ferreira, H.J.C. Froufe, R.M.V. Abreu, A. Martins, M. Pintado

Antimicrobial activity of phenolic compounds identified in wild mushrooms, SAR analysis and docking studies
(Doi.org/)

J. Appl. Microbiol., 115 (2013), pp. 346-357, [10.1111/jam.12196](#) ↗

[View in Scopus](#) ↗ [Google Scholar](#) ↗

[Bae et al., 2020](#) J.W. Bae, H.B. Seo, S. Belkin, M.B. Gu

An optical detection module-based biosensor using fortified bacterial beads for soil toxicity assessment

Anal. Bioanal. Chem., 412 (2020), pp. 3373-3381, [10.1007/s00216-020-02469-z](#) ↗

[View in Scopus](#) ↗ [Google Scholar](#) ↗

[Belkin and Cheng, 2023](#) S. Belkin, J.-Y. Cheng

Miniaturized bioluminescent whole-cell sensor systems

Curr. Opin. Biotechnol., 82 (2023), pp. 1-8, [10.1016/j.copbio.2023.102952](#) ↗

[Google Scholar](#) ↗

[Buchser et al., 2023](#) R. Buchser, P. Sweet, A. Anantharaman, L. Contreras

RNAs as sensors of oxidative stress in bacteria

Annu. Rev. Chem. Biomol. Eng., 14 (2023), pp. 265-281,

[10.1146/annurev-chembioeng-101121-070250](https://doi.org/10.1146/annurev-chembioeng-101121-070250) ↗

[View in Scopus](#) ↗ [Google Scholar](#) ↗

[Caetano et al., 2023](#) A.R. Caetano, R.D. Oliveria, S.P. Celeiro, A.S. Freitas, S.M. Cardoso, S.T.

Goncalves, F. Baltazar, C. Almeida-Aquiar

Phenolic compounds contribution to Portuguese propolis anti-melanoma activity

Molecules, 28 (2023), pp. 1-13, [10.3390/molecules28073107](https://doi.org/10.3390/molecules28073107) ↗

[View in Scopus](#) ↗ [Google Scholar](#) ↗

[Christaki et al., 2012](#) E. Christaki, E. Bonos, I. Giannenas, P. Florou-Paneri

Aromatic plants as a source of bioactive compounds

Agriculture, 2 (2012), pp. 228-243, [10.3390/agriculture2030228](https://doi.org/10.3390/agriculture2030228) ↗

[Google Scholar](#) ↗

[Dhananjaya et al., 2006](#) B.L. Dhananjaya, A. Nataraju, R. Rajesh, C.D.R. Gowda, B.K. Sharath,

B.S. Vishwanath, A. Cletus, J.M. D'Souza

Anticoagulant effect of Naja naja venom 5' nucleotidase: demonstration through the use of novel specific inhibitor, vanillic acid

Toxicon, 48 (2006), pp. 411-421, [10.1016/j.toxicon.2006.06.017](https://doi.org/10.1016/j.toxicon.2006.06.017) ↗



[View PDF](#) [View article](#) [View in Scopus](#) ↗ [Google Scholar](#) ↗

[Duskaev et al., 2023](#) D. Duskaev, M. Kurilkina, O. Zavyalov

Growth-stimulating and antioxidant effects of vanillic acid on healthy broiler chickens

Vet. World, 16 (2023), pp. 518-525

[Crossref](#) ↗ [View in Scopus](#) ↗ [Google Scholar](#) ↗

[Gill and Holley, 2006](#) A.O. Gill, R.A. Holley

Inhibition of membrane bound ATPases of Escherichia coli and Listeria monocytogenes by plant oil aromatics

Int. Food Microbiol., 111 (2006), pp. 170-174, [10.1016/j.ijfoodmicro.2006.04.046](https://doi.org/10.1016/j.ijfoodmicro.2006.04.046) ↗



[View PDF](#) [View article](#) [View in Scopus](#) ↗ [Google Scholar](#) ↗

[Girawale et al., 2022](#) S.D. Girawale, S.N. Meena, V.N. Nandre, S.B. Waghmode, K.M. Kodam

Biosynthesis of vanillic acid by Ochrobactrum anthropi and its applications

Bioorg. Med. Chem., 72 (2022), Article 117000, [10.1016/j.bmc.2022.117000](https://doi.org/10.1016/j.bmc.2022.117000) ↗

 [View PDF](#) [View article](#) [View in Scopus ↗](#) [Google Scholar ↗](#)

[Hajam et al., 2022](#) Y.A. Hajam, R. Rani, S.Y. Ganie

Oxidative Stress in human pathology and aging: molecular mechanisms and perspectives

Cells, 11 (2022), pp. 1-27, [10.3390/cells11030552 ↗](#)

[Google Scholar ↗](#)

[Islas-Flores et al., 2017](#) H. Islas-Flores, L. Manuel Gómez-Oliván, M. Galar-Martínez, E.

Michelle Sánchez-Ocampo, N. Sanjuan-Reyes, M. Ortiz-Reynoso, O. Dublán-García Cyto-genotoxicity and oxidative stress in common carp (*Cyprinus carpio*) exposed to a mixture of ibuprofen and diclofenac

Environ. Toxicol., 32 (2017), pp. 1637-1649, [10.1002/tox.22392 ↗](#)

[View in Scopus ↗](#) [Google Scholar ↗](#)

[Jiang et al., 2017](#) B. Jiang, G. Li, Y. Xing, D. Zhang, J. Jia, Z. Cui, X. Luan, H. Tang

A whole-cell bioreporter assay for quantitative genotoxicity evaluation of environmental samples

Chemosphere, 184 (2017), pp. 384-392, [10.1016/j.chemosphere.2017.05.159 ↗](#)

 [View PDF](#) [View article](#) [View in Scopus ↗](#) [Google Scholar ↗](#)

[Kashyap et al., 2021](#) D. Kashyap, V.K. Garg, N. Goel

Intrinsic and extrinsic pathways of apoptosis: role in cancer development and prognosis

Adv. Protein Chem. Struct. Biol., 125 (2021), pp. 73-95, [10.1016/bs.apcsb.2021.01.003 ↗](#)

[View in Scopus ↗](#) [Google Scholar ↗](#)

[Kaur et al., 2022](#) J. Kaur, M. Gulati, S.K. Singh, *et al.*

Discovering multifaceted role of vanillic acid beyond flavours: nutraceutical and therapeutic potential

Trends Food Scien. Technol., 122 (2022), pp. 187-200, [10.1016/j.tifs.2022.02.023 ↗](#)

 [View PDF](#) [View article](#) [View in Scopus ↗](#) [Google Scholar ↗](#)

[Kessler et al., 2012](#) N. Kessler, J.J. Schauer, S. Yagur-Kroll, S. Melamed, O. Tirosh, S. Belkin, Y. Erel

A bacterial bioreporter panel to assay the cytotoxicity of atmospheric particulate matter

Atmos. Environ., 63 (2012), pp. 94-101, [10.1016/j.atmosenv.2012.09.048 ↗](#)

 [View PDF](#) [View article](#) [View in Scopus ↗](#) [Google Scholar ↗](#)

[Kyselova, 2011](#) Z. Kyselova

Toxicological aspects of the use of phenolic compounds in disease prevention

Inter. Toxicol., 4 (2011), pp. 173-183, [10.2478/v10102-011-0027-5](https://doi.org/10.2478/v10102-011-0027-5) ↗

[View in Scopus](#) ↗ [Google Scholar](#) ↗

[Lou et al., 2011](#) Z. Lou, H. Wang, S. Rao, J. Sun, C. Ma, J. Li

P-Coumaric acid kills bacteria through dual damage mechanisms

Food Control, 25 (2011), pp. 550-554, [10.1016/j.foodcont.2011.11.022](https://doi.org/10.1016/j.foodcont.2011.11.022) ↗

[Google Scholar](#) ↗

[Lu and Gan, 2014](#) Z. Lu, J. Gan

Analysis, toxicity, occurrence and biodegradation of nonylphenol isomers: a review

Environ. Int., 73 (2014), pp. 334-345, [10.1016/j.envint.2014.08.017](https://doi.org/10.1016/j.envint.2014.08.017) ↗



[View PDF](#) [View article](#) [View in Scopus](#) ↗ [Google Scholar](#) ↗

[Maqsood et al., 2014](#) S. Maqsood, S. Benjakul, A. Abushelaibi, A. Alam

Phenolic compounds and plant phenolic extracts as natural antioxidants in prevention of lipid oxidation in sea food: a detailed review

Compreh. Rev. Food Sci. Food Saf., 13 (2014), pp. 1125-1140, [10.1111/1541-4337.12106](https://doi.org/10.1111/1541-4337.12106) ↗

[View in Scopus](#) ↗ [Google Scholar](#) ↗

[Matejczyk et al., 2020c](#) M. Matejczyk, P. Ofman, K. Dąbrowska, R. Świśtocka, W. Lewandowski

Synergistic interaction of diclofenac and its metabolites with selected antibiotics and amygdalin in wastewaters

Environ. Res., 186 (2020), pp. 1095-1111, [10.1016/j.envres.2020.109511](https://doi.org/10.1016/j.envres.2020.109511) ↗

[Google Scholar](#) ↗

[Matejczyk et al., 2020a](#) M. Matejczyk, P. Ofman, K. Dąbrowska, R. Świśtocka, W. Lewandowski

The study of biological activity of transformation products of diclofenac and its interaction with chlorogenic acid

J. Environ. Sci. (China), 91 (2020), pp. 128-141, [10.1016/j.jes.2020.01.022](https://doi.org/10.1016/j.jes.2020.01.022) ↗



[View PDF](#) [View article](#) [View in Scopus](#) ↗ [Google Scholar](#) ↗

[Matejczyk et al., 2020b](#) M. Matejczyk, P. Ofman, K. Dąbrowska, R. Świśtocka, W. Lewandowski

Evaluation of the biological impact of the mixtures of diclofenac with its biodegradation metabolites 4'-hydroxydiclofenac and 5-hydroxydiclofenac on Escherichia coli. DCF synergistic effect with caffeic acid

Arch. Environ. Prot., 46 (2020), pp. 32-53, [10.24425/aep.2020.135760](https://doi.org/10.24425/aep.2020.135760) ↗

[Google Scholar ↗](#)

[Matejczyk et al., 2022](#) M. Matejczyk, P. Ofman, M. Parcheta, R. Świsłocka, W. Lewandowski
The study of biological activity of mandelic acid and its alkali metal salts in wastewaters

Environ. Res., 205 (2022), Article 112429, [10.1016/j.envres.2021.112429 ↗](#)

 [View PDF](#) [View article](#) [View in Scopus ↗](#) [Google Scholar ↗](#)

[Matejczyk et al., 2023](#) M. Matejczyk, P. Ofman, J. Wiater, R. Świsłocka, P. Kondzior, W. Lewandowski

Determination of the effect of wastewater on the biological activity of mixtures of fluoxetine and its metabolite norfluoxetine with nalidixic and caffeic acids with use of E. coli microbial bioindicator strains

Materials, 16 (2023), pp. 1-20, [10.3390/ma16093600 ↗](#)

[Google Scholar ↗](#)

[Melamed et al., 2012](#) S. Melamed, C. Lalush, T. Elad, S. Yagur-Krol, S. Belkin, R. Pedahzur
A bacterial reporter panel for the detection and classification of antibiotic substances: detection and classification of antibiotics

Microbiol. Biotechnol., 5 (2012), pp. 536-548, [10.1111/j.1751-7915.2012.00333 ↗](#)

[View in Scopus ↗](#) [Google Scholar ↗](#)

[Moraskie et al., 2021](#) M. Moraskie, H. Roshid, G. O'Connor, E. Dikici, J.-M. Zingg, S. Deo, S. Daunert

Microbial whole-cell biosensors: current applications, challenges, and future perspectives

Biosens. Bioelectron., 191 (2021), Article 113359, [10.1016/j.bios.2021.113359 ↗](#)

 [View PDF](#) [View article](#) [View in Scopus ↗](#) [Google Scholar ↗](#)

[Mourtzinis et al., 2009](#) I. Mourtzinis, S. Konteles, N. Kalogeropoulos, V.T. Karathanos
Thermal oxidation of vanillin affects its antioxidant and antimicrobial properties

Food Chem., 114 (2009), pp. 791-797, [10.1016/j.foodchem.2008.10.014 ↗](#)

 [View PDF](#) [View article](#) [View in Scopus ↗](#) [Google Scholar ↗](#)

[Muddahally et al., 2023](#) Ch Muddahally, K.Y. Prasad, V.P. Mahendra, P. Ganesan, R. Kumar
Vanillic acid potentiates insulin secretion and prevents pancreatic β -cells cytotoxicity under H₂O₂-induced oxidative stress

Mol. Biol. Rep., 50 (2023), pp. 1311-1320, [10.1007/s11033-022-08046-0 ↗](#)

[Google Scholar ↗](#)

[Oke et al., 2021](#) L.M. Ramorobi, S.S. Mashele, S.L. Bonnet, T.J. Makhafola, K.C. Eze, E.M. Noreljaleel, C.I. Chukwuma
Vanillic acid–Zn(II) complex: a novel complex with antihyperglycaemic and anti-oxidative activity
J. Pharm. Pharmacol., 73 (2021), pp. 1703-1714, [10.1093/jpp/rgab086](#) ↗
[View in Scopus](#) ↗ [Google Scholar](#) ↗

[Pizzino et al., 2017](#) G. Pizzino, N. Irrera, M. Cucinotta
Oxidative Stress: harms and benefits for human health
Oxid. Med. Cel. Longev., 2017 (2017), Article 8416763, [10.1155/2017/8416763](#) ↗
[View in Scopus](#) ↗ [Google Scholar](#) ↗

[Qian et al., 2019](#) W. Qian, Y. Fu, M. Liu, T. Wang, J. Zhang, M. Yang, Z. Sun, X. Li, Y. Li
In vitro antibacterial activity and mechanism of vanillic acid against carbapenem-resistant Enterobacter cloacae
Antibiotics, 13 (8) (2019), p. 220, [10.3390/antibiotics8040220](#) ↗
[View in Scopus](#) ↗ [Google Scholar](#) ↗

[Rahman et al., 2022](#) M. Rahman, S. Rahaman, R. Islam
Role of phenolic compounds in human disease: current knowledge and future prospects
Molecules, 27 (2022), pp. 1-36, [10.3390/molecules27010233](#) ↗
[View in Scopus](#) ↗ [Google Scholar](#) ↗

[Ramos et al., 2023](#) L.F. Ramos, J. Pluschke, A.M. Bernardes, S.-U. Greißen
Polyphenols in food processing wastewaters: A review on their identification and recovery
Clean. Circ. Bioecon., 5 (2023), pp. 1-24, [10.1016/j.clcb.2023.100048](#) ↗
[Google Scholar](#) ↗

[Rojas-Villacorta et al., 2022b](#) W. Rojas-Villacorta, S. Rojas-Flores, M. De La Cruz-Noriega, H.C. Espino, F. Diaz, M.G. Cardenas
Microbial biosensors for wastewater monitoring: mini review
Processes, 10 (2022), pp. 2-13, [10.3390/pr10102002](#) ↗
[Google Scholar](#) ↗

[Rojas-Villacorta et al., 2022a](#) W. Rojas-Villacorta, S. Rojas-Flores, M. De La Cruz-Noriega, H. Chinchay Espino, F. Diaz, M. Gallozzo Cardenas
Microbial biosensors for wastewater monitoring: mini-review
Processes, 10 (2022), pp. 2-13, [10.3390/pr10102002](#) ↗
[Google Scholar](#) ↗

[Sazykin I.S. and Sazykin M.A. 2023](#)

The role of oxidative stress in genome destabilization and adaptive evolution of bacteria

Gene, 20 (2023), pp. 1-13, [10.1016/j.gene.2023.147170](#) ↗

[Google Scholar](#) ↗

[Schieber and Chandel, 2014](#) M. Schieber, N.S. Chandel

ROS function in redox signaling and oxidative stress

Curr. Biol., 19 (24) (2014), pp. 1-41, [10.1016/j.cub.2014.03.034](#) ↗

[View in Scopus](#) ↗ [Google Scholar](#) ↗

[Seixas et al., 2022](#) A.F. Seixas, A.P. Quendera, J.P. Sousa, A.F.Q. Silva, C.M. Arraiano, J.M. Andrade

Bacterial response to oxidative stress and RNA oxidation

Front. Genet., 12 (2022), pp. 8215-8235, [10.3389/fgene.2021.821535](#) ↗

[Google Scholar](#) ↗

[Sha et al., 2023](#) Y. Sha, L. Zhou, Z. Wang, Y. Ding, M. Lu, Z. Xu, R. Zhai, M. Jin

Adaptive laboratory evolution boosts *Yarrowia lipolytica* tolerance to vanillic acid

J. Biotechnol., 367 (2023), pp. 42-52, [10.1016/j.jbiotec.2023.03.006](#) ↗



[View PDF](#) [View article](#) [View in Scopus](#) ↗ [Google Scholar](#) ↗

[Shabani et al., 2023](#) M. Shabani, Z. Jamali, D. Bayrami, A. Salimi

Vanillic acid alleviates methamphetamine-induced mitochondrial toxicity in cardiac mitochondria via antioxidant activity and inhibition of MPT pore opening: an in vitro study

BMC Pharmacol. Toxicol., 24 (2023), pp. 1-11, [10.1186/s40360-023-00676-9](#) ↗

[View in Scopus](#) ↗ [Google Scholar](#) ↗

[Świśtocka et al., 2013](#) R. Świśtocka, J. Piekut, W. Lewandowski

The relationship between molecular structure and biological activity of alkali metal salts of vanillic acid: spectroscopic, theoretical and microbiological studies

Spectrochim. Acta A: Mol. Biomol. Spectrosc., 100 (2013), pp. 31-40,

[10.1016/j.saa.2012.01.044](#) ↗



[View PDF](#) [View article](#) [View in Scopus](#) ↗ [Google Scholar](#) ↗

[Tanaka et al., 2019](#) T. Tanaka, H. Onuma, T. Shigihara, E. Kimura, Y. Fukuta

Anti-osteoporotic effects of syringic acid and vanillic acid in the extracts of waste beds after mushroom cultivation

J. Biosci. Bioeng., 128 (2019), pp. 622-629, [10.1016/j.jbiosc.2019.04.021](https://doi.org/10.1016/j.jbiosc.2019.04.021) ↗



[View PDF](#) [View article](#) [View in Scopus](#) ↗ [Google Scholar](#) ↗

[Trombetta et al., 2005](#) D. Trombetta, F. Castelli, M.G. Sarpietro, V. Venuti, M. Cristani, C. Daniele, A. Saija, G. Mazzanti, G. Bisignano

Mechanisms of antibacterial action of three monoterpenes

Antimicrob. Agents Chemother., 49 (2005), pp. 2474-2478,

[10.1128/AAC.49.6.2474-2478.2005](https://doi.org/10.1128/AAC.49.6.2474-2478.2005) ↗

[View in Scopus](#) ↗ [Google Scholar](#) ↗

[Tu et al., 2022](#) N. Tu, H. Liu, W. Li, S. Yao, J. Liu, Z. Guo, R. Yu, H. Du, J. Li

Quantitative structure-toxicity relationships of halobenzoquinone isomers on DNA reactivity and genotoxicity

Chemosphere, 309 (2022), Article 136763, [10.1016/j.chemosphere.2022.136763](https://doi.org/10.1016/j.chemosphere.2022.136763) ↗



[View PDF](#) [View article](#) [View in Scopus](#) ↗ [Google Scholar](#) ↗

[Victor-Ortega et al., 2022](#) M.D. Victor-Ortega, A.S. Fajardo, D. Airado-Rodriguez

Sustainable development: use of agricultural waste materials for vanillic acid recovery from wastewater

Sustainability, 14 (2022), pp. 2818-2827, [10.3390/su14052818](https://doi.org/10.3390/su14052818) ↗

[View in Scopus](#) ↗ [Google Scholar](#) ↗

[Wang et al., 2018](#) H. Wang, E. Chambers, J. Kan

Sensory characteristics of combinations of phenolic compounds potentially associated with smoked aroma in foods

Molecules, 23 (2018), pp. 1867-1878, [10.3390/molecules23081867](https://doi.org/10.3390/molecules23081867) ↗

[View in Scopus](#) ↗ [Google Scholar](#) ↗

[Yanez et al., 2016](#) E. Yanez, P. Santander, D. Contreras, J. Yanez, L. Cornejo, H.D. Mansilla

Homogeneous and heterogeneous degradation of caffeic acid using photocatalysis driven by UVA and solar light

J. Environ. Sci. Health A Tox. Hazard. Subst. Environ. Eng., 51 (2016), pp. 78-85,

[10.1080/10934529.2015.1086211](https://doi.org/10.1080/10934529.2015.1086211) ↗

[View in Scopus](#) ↗ [Google Scholar](#) ↗

[Yin et al., 2022](#) J. Yin, Y. Zhu, Y. Liang, Y. Luo, J. Lou, X. Hu, Q. Meng, T. Zhu, Z. Yu

Development of whole-cell biosensors for screening of peptidoglycan-targeting antibiotics in a Gram-negative bacterium

Appl. Environ. Microbiol., 22 (2022), pp. 1-14, [10.1128/aem.00846-22](https://doi.org/10.1128/aem.00846-22) ↗

[Google Scholar](#) ↗

[Zappi et al., 2021](#) D. Zappi, E. Coronado, V. Soljan, G. Basile, G. Varani, M. Turems, M.T. Giardi

A microbial sensor platform based on bacterial bioluminescence (luxAB) and green fluorescent protein (gfp) reporters for in situ monitoring of toxicity of wastewater nitrification process dynamics

Talanta, 221 (2021), pp. 1-8, [10.1016/j.talanta.2020.121438](https://doi.org/10.1016/j.talanta.2020.121438) ↗

[Google Scholar](#) ↗

[Zhu et al., 2022](#) Y. Zhu, E. Elcin, M. Jiang, B. Li, H. Wang, X. Zhang, Z. Wang
Use of whole-cell bioreporters to assess bioavailability of contaminants in aquatic systems

(Doi: doi.org/)

Front. Chem., 10 (2022), p. 1018124, [10.3389/fchem.2022.1018124](https://doi.org/10.3389/fchem.2022.1018124) ↗

[View in Scopus](#) ↗ [Google Scholar](#) ↗

[Zilius et al., 2013](#) M. Zilius, K. Ramanauskiene, V. Briedis
Release of propolis phenolic acids from semisolid formulations and their penetration into the human skin in vitro

Evid. Based Complement Altern. Med., 2013 (2013), Article 958717, [10.1155/2013/958717](https://doi.org/10.1155/2013/958717) ↗

[View in Scopus](#) ↗ [Google Scholar](#) ↗

Cited by (0)

© 2024 The Authors. Published by Elsevier Inc.



All content on this site: Copyright © 2024 Elsevier B.V., its licensors, and contributors. All rights are reserved, including those for text and data mining, AI training, and similar technologies. For all open access content, the Creative Commons licensing terms apply.

